

Binol Quinone Methides as Bisalkylating and DNA Cross-Linking Agents

Sara N. Richter,[†] Stefano Maggi,[‡] Stefano Colloredo Mels,[‡] Manlio Palumbo,[†] and Mauro Freccero^{*‡}

Contribution from the Dipartimento di Chimica Organica, Università di Pavia, Via le Taramelli 10, 27100 Pavia, Italy, and Dipartimento di Scienze Farmaceutiche, Università di Padova, Via Marzolo 5, 35131 Padova, Italy

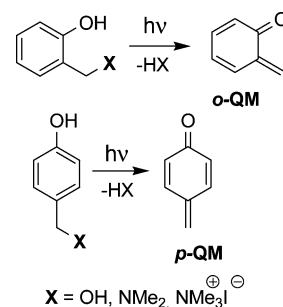
Received April 23, 2004; E-mail: mauro.freccero@unipv.it

Abstract: The photogeneration and detection of new binol quinone methides undergoing mono- and bisalkylation of free nucleophiles was investigated by product distribution analysis and laser flash photolysis in water solution using binol quaternary ammonium derivatives **2** and **12** as photoactivated precursors. The alkylation processes of N and S nucleophiles are strongly competitive with the hydration reaction. DNA cross-linking potency of the water-soluble binol quaternary ammonium salt **2** was investigated as a pH function and compared to that of other quaternary ammonium salts capable of benzo-QM (QM = quinone methide) photogeneration by gel electrophoresis. DFT calculations in the gas phase and in water bulk on the binol and benzo quaternary ammonium salts **2** and **4** evidence structural and electrostatic features of the binol derivative which might offer a rationalization of its promising high photo-cross-linking efficiency.

Introduction

In recent years there has been increasing interest in the design of chemical agents capable of inducing DNA interstrand cross-linking (ISC), which, shutting down the DNA replication process, represents by far the most cytotoxic of all the alkylation events.¹ Among the compounds capable of DNA ISC, the photoactivated agents are probably the least developed class, with the exception of psoralens.² Quinone methides (QMs) have been successfully used to accomplish nucleoside alkylation and DNA ISC by photochemical³ and fluoride-induced⁴ activation. Wan,⁵ Kresge,⁶ Saito,⁷ and our group⁸ described the photogeneration of *o*-QM and *p*-QM (Scheme 1) starting, respectively, from benzyl alcohols (X = OH)^{5,6} and Mannich bases⁷ (X = NMe₂) and their ammonium salts⁸ (X = NMe₃⁺I⁻) in water.

Scheme 1



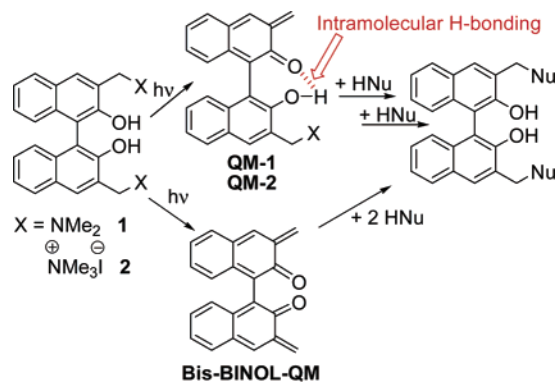
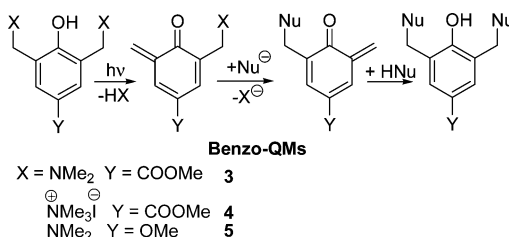
We have recently shown that benzylammonium salts of phenolic Mannich bases (Scheme 1, X = NMe₃⁺) are better and preferable QM precursors than both the above, since they display (i) a higher photochemical quantum yield ($\Phi = 0.98$) than the alcohols ($\Phi = 0.23$), (ii) a much higher water solubility, and (iii) no nucleophilicity, unlike the Mannich bases. The latter feature protects the precursor from alkylation reaction by the photogenerated QM. Our activation protocol⁸ has been applied very recently by Zhou for the generation of a bisalkylating QM with a biphenyl structure capable of a mild and efficient DNA ISC.⁹ These results prompted us to report our initial data on two new potential photoinducible bisalkylating agents, the amine **1** and its quaternary ammonium salt **2** (Scheme 2). We have chosen to investigate the photoactivation and the reactivity of the binol quaternary ammonium **2** as the precursor of a bisalkylating agent for the reasons discussed below.

[†] Università di Padova.

[‡] Università di Pavia.

- (1) Rajski, S. R.; Williams, R. M. *Chem. Rev.* **1998**, *98*, 2723–2795.
- (2) Cimino, G. D.; Gamper, H. B.; Isaacs, S. T.; Hearst, J. E. *Annu. Rev. Biochem.* **1985**, *54*, 1151–1193.
- (3) Chatterjee, M.; Rokita, S. E. *J. Am. Chem. Soc.* **1994**, *116*, 1690–1697.
- (4) (a) Zeng, Q.; Rokita, S. E. *J. Org. Chem.* **1996**, *61*, 9080–9081. (b) Yang, J.; Pande, P.; Shearer, J.; Greenberg, W. A.; Zeng, Q.; Rokita, S. E. *J. Org. Chem.* **1997**, *62*, 3010–3012. (c) Pande, P.; Shearer, J.; Yang, J.; Greenberg, W. A.; Rokita, S. E. *J. Am. Chem. Soc.* **1999**, *121*, 6773–6779. (d) Veldhuyzen, W. F.; Shallop, A. J.; Jones, R. A.; Rokita, S. E. *J. Am. Chem. Soc.* **2001**, *123*, 11126–11132. (e) Zanaletti, R.; Freccero, M. *Chem. Commun.* **2002**, 1908–1909.
- (5) (a) Wan, P.; Barker, B.; Diao, L.; Fisher, M.; Shi, Y.; Yang, C. *Can. J. Chem.* **1996**, *74*, 465–475. (b) Diao, L.; Cheng, Y.; Wan, P. *J. Am. Chem. Soc.* **1995**, *117*, 5369–5370. (c) Brousmiche, D.; Wan, P. *Chem. Commun.* **1998**, 491–492.
- (6) (a) Chiang, Y. A.; Kresge, J.; Zhu, Y. *J. Am. Chem. Soc.* **2002**, *123*, 6349–6356. (b) Chiang, Y. A.; Kresge, J.; Zhu, Y. *J. Am. Chem. Soc.* **2002**, *123*, 717–722. (c) Chiang, Y. A.; Kresge, J.; Zhu, Y. *J. Am. Chem. Soc.* **2001**, *123*, 8089–8094.
- (7) Nakatani, K.; Higashida, N.; Saito, I. *Tetrahedron Lett.* **1997**, *38*, 5005–5008.
- (8) Modica, E.; Zanaletti, R.; Freccero, M.; Mella, M. *J. Org. Chem.* **2001**, *66*, 41–52.

- (9) Wang, P.; Liu, R.; Wu, X.; Ma, H.; Cao, X.; Zhou, P.; Zhang, J.; Weng, X.; Zhang, X.-L.; Qi, J.; Zhou, X.; Weng L. *J. Am. Chem. Soc.* **2003**, *125*, 1116–1117.

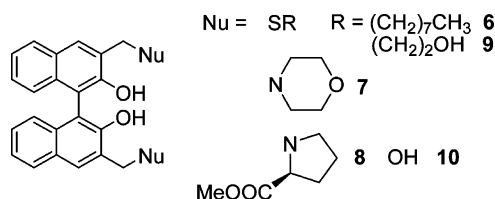
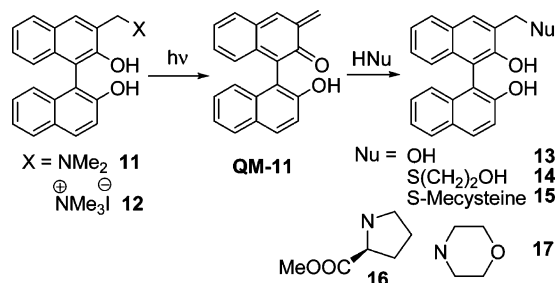
Scheme 2. Generation and Reactivity of Binol-QMs **QM-1** and **QM-2****Scheme 3.** Tandem Quinone Methide Generation of Benzo-QMs

The proximity of the two 2,2'-hydroxy groups could provide intramolecular general-acid catalysis for enhancing the reactivity of transient binol-QMs **QM-1** and **QM-2** in Scheme 2. In fact, it is well-known that the reactivity and selectivity of QMs in alkylation reactions can be enhanced by specific-acid^{5,6,8} and general-acid¹⁰ catalysis. The latter is particularly effective when strong intramolecular hydrogen bonding involving the QM carbonyl oxygen is operative.¹¹ Moreover, derivatives **1** and **2** exist as stable, not interconvertible, enantiomers (unlike biphenyl derivatives), and this could represent an opportunity to explore the effect of the axial chirality on the potency of the enantiopure precursor of cross-linking agents.¹²

This study is part of a more comprehensive study aimed at exploiting the promising features of derivatives **1** and **2** as precursors of a bisalkylating binol-QM, and it will be focused on the photoactivation of **1** and **2** as racemates by UV-vis irradiation. In addition, we will also compare the ISC potency of **2** to that of a few benzo derivatives such as **3–5** (Scheme 3), which are precursors of benzo-QMs. The latter substrates, according to Rokita, are able to induce DNA cross-linking through a “tandem quinone methide generation” (Scheme 3).^{4a}

Results and Discussion

Photogeneration and Reactivity of Binol-QMs. The amine precursors **1**, **3**, and **5** used for the photogeneration of the alkylating species have been synthesized by Mannich reactions using (isobutoxymethyl)dimethylamine at 160 °C in isobutanol, or *N,N*-dimethylmethyleniminium chloride. Quaternarization was achieved using methyl iodide. To test the possibility of using **1** and **2** as formal precursors of a bisalkylating QM, we

Chart 1**Scheme 4.** Generation and Reactivity of Monoalkylating **QM-11**

explored the photoreactivity of **1** and **2** as racemates.¹² The binol-QMs were photogenerated at $\lambda \geq 360$ nm and trapped in organic solvent and in water by N, O, and S nucleophiles. Photolysis of **1** [10^{-3} M, in a photoreactor with four lamps (15 W), 310 and 360 nm, ca. 25 °C, 10 and 25 min, under an O_2 -purged solution] in CH_2Cl_2 with octane-1-thiol, morpholine, and L-proline methyl ester, at a 10^{-2} M concentration, gave the corresponding bisalkylated adducts **6–8** (Chart 1) in quantitative yields. Photolysis of **2** in a water solution containing morpholine and mercaptoethanol ($[\text{HNu}] = 5 \times 10^{-2}$ M) similarly afforded the adducts **7** and **9** in $\geq 70\%$ yields, accompanied by small amounts ($\leq 20\%$) of alcohol **10**. Precursors **1–5** and alkylation adducts **6–10** have been purified and characterized. Monoalkylated adducts were not detected by HPLC, and therefore, if they formed at all, their yields were very low (i.e., $< 5\%$).

To clarify the first alkylation event of our bisalkylating agents, we investigated (i) the product distribution of the alkylation reaction by **11** and **12** using the same nucleophiles and (ii) the formation of transient alkylating species by laser flash photolysis (LFP). The irradiation of the monoalkylating binol derivatives **11** and **12** was carried out under the same conditions described above for the bisalkylating binol derivatives **1** and **2** in the presence of the same nucleophiles at identical concentrations, efficiently obtaining the adducts **13–17** (Scheme 4), both in CH_2Cl_2 and in water.

Detection and Lifetime of Transient Binol-QMs by Laser Flash Photolysis. We have shown previously that LFP provides an effective method for direct detection of QMs, starting from quaternary ammonium salts of Mannich bases.⁸ LFP of **2** and **12** ($\lambda_{\text{exc}} = 266$ nm, Nd:YAG laser, < 10 mJ per pulse) in oxygen-purged aqueous solutions yielded two transient species with $\lambda_{\text{max}} = 380$ and 360 nm, respectively (see Figure 1). These transients were confidently assigned to the binol-QM structures **QM-2** (Scheme 2) and **QM-11** (Scheme 4) on the basis of (i) the spectroscopic similarity of their transient spectra (Figure 1), (ii) the similar maximum absorbance of the parent 2,3-naphtho-QM ($\lambda_{\text{max}} = 395.5$ nm),¹³ and (iii) trapping experiment results. In fact, after 30–40 laser shots (8 mJ power), **10** and **13** were detected by HPLC in flashed aqueous solutions of **2**

(10) (a) Freccero, M.; Di Valentin, C.; Sarzi-Amadè, M. *J. Am. Chem. Soc.* **2003**, *125*, 3544–3553. (b) Freccero, M.; Gandolfi, R.; Sarzi-Amadè, M. *J. Org. Chem.* **2003**, *68*, 6411–6423. (c) Di Valentin, C.; Freccero, M.; Zanaletti, R.; Sarzi-Amadè, M. *J. Am. Chem. Soc.* **2001**, *123*, 8366–8377.

(11) Lewis, M. A.; Graff Yoerg, D.; Bolton, J. L.; Thompson, J. A. *Chem. Res. Toxicol.* **1996**, *9*, 1368–1374.

(12) Ionic strength effects on both the reactivity of enantiopure **2** and its XL potency are under investigation.

(13) Musil, L.; Koutek, B.; Pisova, M.; Soucek, M. *Collect. Czech. Chem. Commun.* **1981**, *46*, 1148–1159.

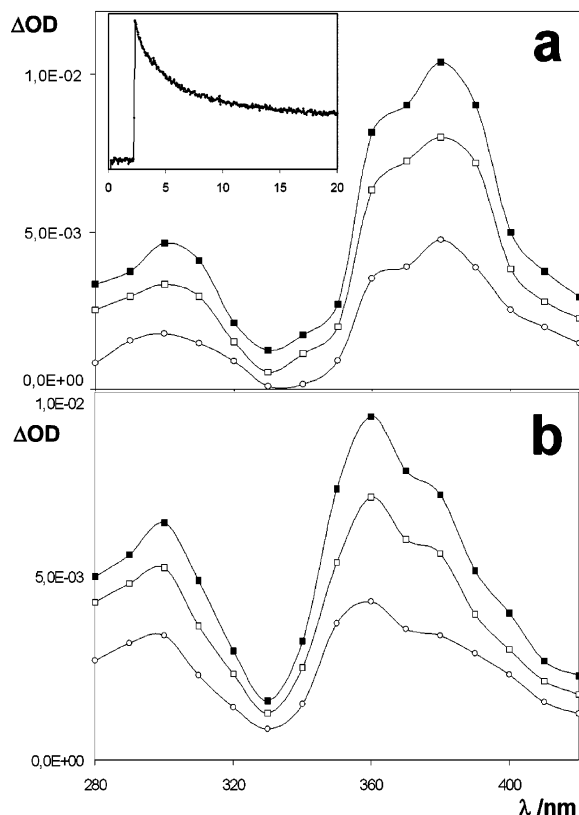


Figure 1. Transient absorptions upon flashing binol quaternary ammonium salts **2** (a) and **12** (b) in water. Inset: decay of the absorption at 380 nm for **QM-2**, time unit 5 μ s/division.

and **12**, respectively, as the main products. In the presence of 2-mercaptoethanol, the corresponding alkylation adducts **9** and **14** were identified by comparison with authentic samples obtained from photochemical preparative experiments as described above.

Both these transients react very fast with water ($k_2 = 4.7 \times 10^3$ and $10.6 \times 10^3 \text{ M}^{-1} \text{ s}^{-1}$ for **QM-1** and **QM-11**, respectively) and with mercaptoethanol ($k_2 = 5.5 \times 10^6$ and $2.5 \times 10^7 \text{ M}^{-1} \text{ s}^{-1}$) at 25 $^\circ\text{C}$, displaying an intermediate reactivity between that of the parent *o*-quinone methide (*o*-QM)^{5,6,8} and the stabilized benzyl carbocations.¹⁴ Their lifetime was unaffected by the presence of oxygen, in accordance with what has been reported by Wan^{5b} and us⁸ for the prototype *o*-QM. All of these characteristics closely matched those typical of QMs. In addition, the similarity between spectroscopic and kinetic properties of the two transient species rules out the possibility of a photochemical generation, in a single step, of a bis(quinone methide) as a real intermediate (**Bis-BINOL-QM**, Scheme 2).

Cross-Linking Experiments. The good solubility of **2** in water ($3.3 \times 10^{-2} \text{ M}$) allowed testing it as a DNA cross-linking agent under aqueous conditions. Comparison of **2** to **3–5**, conveniently absorbing at similar wavelengths, allows an evaluation of the relative cross-linking potency, reducing the effects due to poor absorption.

The DNA–DNA cross-linking ability of compounds **2–5** was investigated using a negatively supercoiled plasmid DNA (pBR322) in an alkaline agarose gel assay.¹⁵ DNA cross-linking

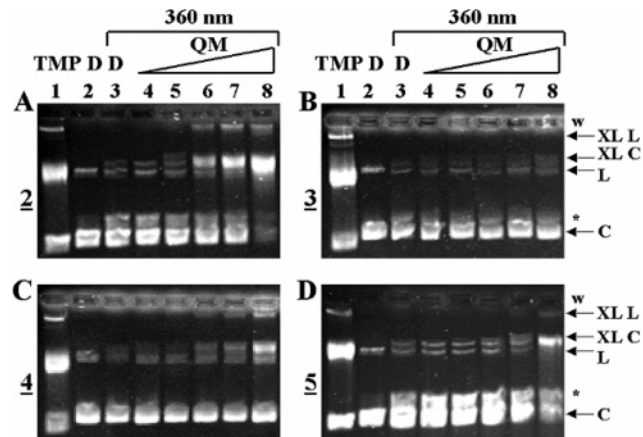


Figure 2. DNA cross-linking (XL) activity: (A–D) concentration-dependent activity of compounds **2–5**, respectively. Plasmid DNA was mixed with increasing amounts (0.5, 1, 5, 10, and 50 μM) of each compound (lanes 4–8) in phosphate buffer (50 mM, pH 7.5). Reaction mixtures were irradiated at 360 nm for 30 min and loaded onto a 1% alkaline agarose gel. Gels were stained with ethidium bromide. “D” indicates DNA samples, lacking compounds: lane 2 is nontreated and nonirradiated DNA, and lane 3 is nontreated, irradiated DNA. Lane 1 is a control for XL species induced by 4,5',8-trimethylpsoralen (TMP) at 360 nm. Nonreacted circular and linear forms of plasmid are indicated as “C” and “L”; XL species derived from circular and linear plasmid are indicated as “XL C” and “XL L”, respectively, on the right side of the figure. The asterisk indicates lower mobility DNA species due to DNA self-alkylation, which generates thymine dimers by UV irradiation.¹⁶ “w” stands for wells.

(XL) experiments were initially carried out in phosphate-buffered solutions at pH 7.5. Samples were irradiated at 360 nm in the same photoreactor used for the preparative experiments. Nonirradiated DNA and irradiated DNA without precursors or with psoralen were used as controls. The results and concentration dependence for compounds **2–5** at pH 7.5 are depicted in Figure 2.

Binol derivative **2** induces detectable cross-links (XL C and XL L) of both the circular (C) and linear (L) forms of the plasmid at concentrations as low as 1–5 μM (Figure 2A, lanes 5 and 6, XL C and XL L), and produces 90% cross-linking at 50 μM (Figure 2A, lane 8). Benzo derivative **4** also stimulates XL at low micromolar concentrations, but the overall effect is lower than that of **2**, the amount of XL plasmid being around 45% at 50 μM . Benzo derivatives **3** and **5** are at least 100-fold less potent than **2** and **4**, since they display detectable cross-links only at a 50 μM concentration (Figure 2B,D, lanes 8). The enhanced potency of **4** in comparison to the corresponding amine **3** by 2 orders of magnitude was unexpected, since we had shown previously that the amine and quaternary ammonium salt used for the photogeneration of the prototype benzo-*o*-QM display the very same photochemical quantum yield in the generation of QM under neutral and slightly basic conditions.⁸

To test the effect of pH on the potency of **3** and **4**, the two compounds were assayed in phosphate-buffered solutions at increasing pH values (6.5, 7.5, and 8.8). As shown in Figure 3C, the cross-linking efficiency of **4** is highest at pH 6.5 and gradually decreases at increasing pH values (Figure 3C, lanes 2–4). The reverse is true for **3**, the activity of which is slightly better at pH 8.8 (Figure 3B, lanes 2–4). Interestingly, XL effects of **3** and **4** are entirely comparable at pH 8.8, where **4** is mainly in the phenoxide form (monocationic), paralleling the data on

(14) (a) Toteva M. M.; Moran, M.; Amyes T. L.; Richard J. P. *J. Am. Chem. Soc.* **2003**, *125*, 8814–8819. (b) Richard, J. P.; Toteva, M. M.; Crueiras, J. J. *Am. Chem. Soc.* **2000**, *122*, 1664–1674.

(15) McDonell, M. W.; Simon, M. N.; Studier, F. W. *J. Mol. Biol.* **1977**, *110*, 119–146.

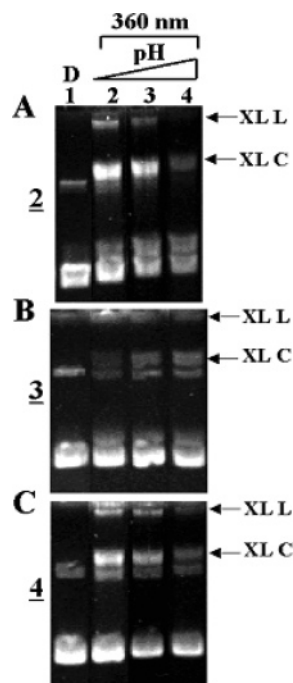


Figure 3. (A–C) pH-dependent activity of compounds 2–4. Plasmid DNA and 2, 3, or 4 (50 μ M) were irradiated at 360 nm for 30 min in phosphate buffer at pH 6.5 (lanes 2), 7.5 (lanes 3), and 8.8 (lanes 4). Lane 1 is a control for nonirradiated and nontreated DNA.

the photochemical quantum yield in the generation of QM. The same behavior observed for 4, i.e., the highest activity at lower pH, is observed for 2 (Figure 3A).

The above evidence indicates that the quaternary ammonium salts 2 and 4 display higher potency in their biscationic forms,¹⁷ and this may be the result of an electrostatic preassociation of the QM precursors 2 and 4 to the anionic DNA phosphate backbone.

Finally, cross-linking activities of compounds 2–4 (10 and 100 μ M) were compared after irradiation at 360 and 310 nm in phosphate buffer (pH 7.5) (Figure 4). Nonirradiated DNA and irradiated DNA without drugs or with psoralen were used as controls. Though DNA irradiated at 310 nm undergoes a higher photochemical degradation compared to DNA irradiated at 360 nm (Figure 4, lanes 4 and 3, respectively),^{18–20} it is still possible to compare drug-induced cross-linking effects. 2, 4, and 5 clearly exhibit around 30–50% higher cross-linking at 360 nm than at 310 nm (Figure 4; compare lanes 5 and 6, 13 and 14, and 17 and 18 with lanes 7 and 8, 15 and 16, and 19 and 20, respectively). On the contrary, 3 displays a 40% increased activity at 310 nm (Figure 4; compare lanes 9 and 10 with lanes 11 and 12).

(16) Formation of DNA monoalkylation products has been suggested by a reviewer as another reasonable cause for the generation of the smear bands indicated by an asterisk in the gel electrophoresis reported in Figure 2. We believe that such a band should be mainly attributed to the dimeric pyrimidine lesions (ref 29) by UV irradiation as suggested by the presence of a similar band in the gel of an irradiated DNA sample lacking alkylating agents (Figure 2A,D, lanes 3). Nevertheless, the reviewer's hypothesis cannot be completely ruled out because the intensity of the band arising from the irradiation of DNA on its own is weaker than that of the band obtained in the presence of the XL agents. This evidence is particularly true for the benzo derivative 5.

(17) Estimated $pK_a(2) \leq 8.7$ from similar structures: Epstein, J.; Plapinger, R. E.; Michel, H. O.; Cable, J. R.; Stephani, R. A.; Hester R. J.; Billington, C., Jr.; List G. R. *J. Am. Chem. Soc.* **1964**, *86*, 3075–3084.60

(18) Freeman, S. E.; Ryan, S. L. *Mutat. Res.* **1990**, *235*, 181–186.

(19) Walker, I. G.; Sridhar, R. *Chem.-Biol. Interact.* **1976**, *12*, 229–239.

(20) Nes, I. F. *Nucleic Acids Res.* **1980**, *8*, 1575–1589.

These data are consistent with the location of the compound absorption maximum, which is close to 360 nm for 2, 4, and 5, while it is around 310–320 nm for 3. In particular, the absorption spectrum of 3 shifts toward 360 nm when the phenolic hydroxyl group is deprotonated, and this fact accounts for the enhanced activity of 3 at higher pH (Figure 3B).

Computational Results. We investigated the conformational profile of (*S*)-2,2'-dihydroxy-3,3'-bis[(trimethylammonium)methyl]-1,1'-binaphthyl and 3,5-bis[(trimethylammonium)methyl]-4-hydroxybenzene, which are the cations of the ionic reactants 2 and of the *para*-unsubstituted analogue of 4 (4H), respectively (Scheme 3, Y = H). The computation has been performed in the gas phase and in water bulk using the hybrid density functional method B3LYP with the 6-31G(d) basis set and C-PCM solvation model. Two minima were located on the conformational potential energy surface of the cation of reactant 2 (i.e., 2a and 2b, Figure 5). In conformer 2a, the CH₂–NMe₃ bond on the B naphthyl ring points away from the reader, below the plane of the B aromatic ring, while in the other conformer, 2b, the same bond points toward the reader, above the naphthyl ring.

Computational data display that (i) the two conformers 2a and 2b have comparable stability in water (with 2b being only 0.8 kcal/mol more stable than 2a) and that (ii) the dipole moment of 2 ($\mu = 19.9$ D for conformer 2a and $\mu = 17.0$ D for 2b) is much higher than the dipole moment of 4H ($\mu = 4.3$ D) in water solution. Such a huge difference in the dipolar properties arises from the geometrical differences between 2 and 4H. In fact, the two most stable conformers 2a and 2b keep the cationic quaternary ammonium branches on the same side of the molecule with the polarizable binaphthyl moiety on the other side. From an electrostatic point of view such a geometric array gives rise to a molecule which looks like a long dipole. In contrast, due to steric hindrance, 4H shows the cationic quaternary ammonium branches on opposite sides, with the less polarizable benzene ring located in the middle.

Hence, the remarkable difference in DNA cross-linking potency between the binol derivative 2 and the most potent precursor of benzo-QMs (4) is likely caused by a combination of the unique features of salt 2 (i.e., axial chirality, dicationic and strong dipolar characters), and not by formation of a bis-(quinone methide) intermediate, as shown previously by LFP transient detection. These aspects may cooperate in establishing a binding ability to the DNA anionic phosphate backbone before photoactivation.¹²

Conclusion

In conclusion, we have shown the formation of a new and detectable binol-QM capable of undergoing bisalkylation in water and DNA ISC with promising potency by UV–vis photoactivation of the bis(quaternary ammonium salt) 3,3'-bis-(trimethylaminomethyl)-binol (2). The correlations between the above structural key features of 2 and its potency as a DNA cross-linking agent are currently under investigation.

Experimental Section

General Procedures. The amines 1,²¹ 3,²² and 5²³ have been prepared according to published procedures. The amines 1, 3, and 5 have been previously characterized. The quaternary ammonium salts

(21) Kitajima, H.; Ito, K.; Katsuki, T. *Tetrahedron* **1997**, *53*, 17015–17028.

(22) Bengs, W.; Friedrich, K. *Chem. Ber.* **1956**, *89*, 1208–1209.

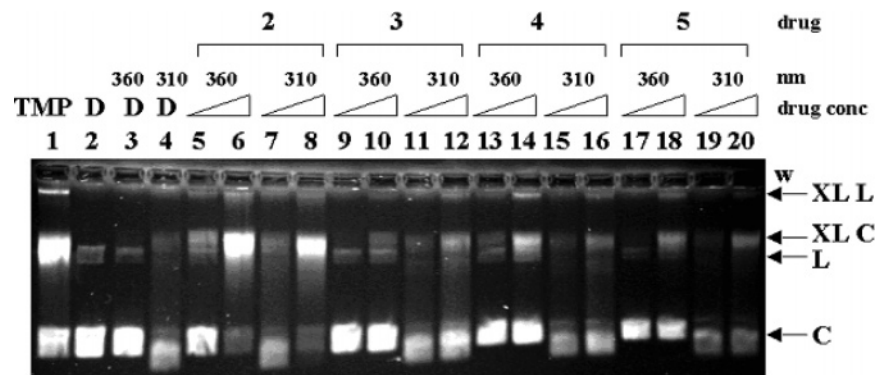


Figure 4. Wavelength-dependent DNA cross-linking activity. Plasmid DNA and **2** (lanes 5–8), **3** (lanes 9–12), **4** (lanes 13–16), and **5** (lanes 17–20) at concentrations of 10 μM (odd lanes 5–20) and 100 μM (even lanes 5–20) were irradiated at 360 nm (lanes 5, 6, 9, 10, 13, 14, 17, and 18) or at 310 nm (lanes 7, 8, 11, 12, 15, 16, 19, and 20) for 30 min in phosphate buffer at pH 7.5. Lane 2 is nontreated and nonirradiated DNA; lanes 3 and 4 are nontreated DNA irradiated at 360 and 310 nm, respectively. Lane 1 is a control for cross-linked species induced by 4,5',8-trimethylpsoralen at 360 nm. Nonreacted circular and linear forms of plasmid are indicated as “C” and “L”; cross-linked species derived from circular and linear plasmid are indicated as “XL C” and “XL L”, respectively, on the right of the gel. “w” stands for wells.

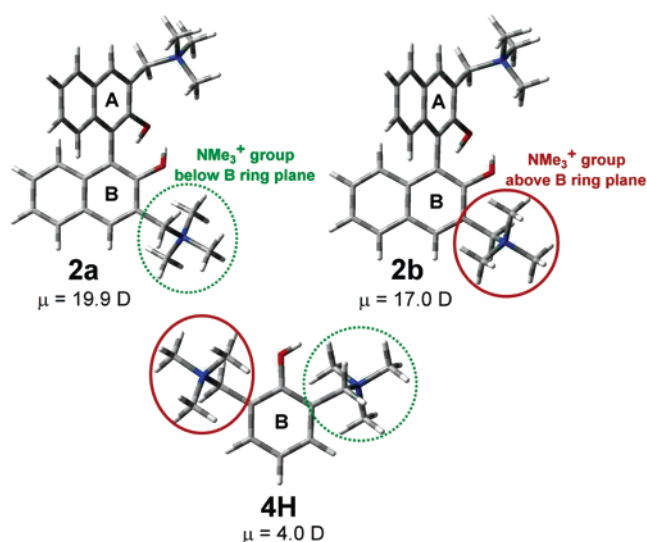


Figure 5. Geometries of conformers **2a** and **2b** and of **4H**, in water solution, at the B3LYP-C-PCM/6-31G(d) level of theory.

2, **4**, and **12** have been synthesized by *N*-methylation from the corresponding amines, and were unknown compounds, like the amine **11**. The other reagents (of commercial origin) were distilled or recrystallized before use. For the irradiations, spectroscopic grade solvents were used as received.

^1H and ^{13}C NMR spectra were recorded with a 300 MHz spectrometer, and the chemical shifts are reported relative to the peak for TMS. The structures of new compounds were deduced from the results of ^1H , ^{13}C , DEPT-135, and 2D correlated experiments. Reaction products were separated and quantified analytically by reversed-phase (Intersil ODS-2, 5 μm , column dimensions $\varnothing = 4.6$ mm, length = 250 mm and $\varnothing = 10.0$ mm, length = 250 mm, Micro-Column) HPLC chromatography using a variable-wavelength detector.

Racemic 2,2'-Dihydroxy-3,3'-bis[(trimethylammonium iodide)methyl]-1,1'-binaphthyl (2). Racemic **2** was prepared, in almost quantitative yield, from 2,2'-dihydroxy-3,3'-bis(dimethylaminomethyl)-1,1'-binaphthyl (**1**). The Mannich base (0.5 g, 1.25 mmol) was treated with methyl iodide (0.5 mL) in CHCl_3 (8 mL). After the mixture was stirred for 12 h at room temperature, the insoluble quaternary am-

monium salt was filtered. Mp: >210 $^\circ\text{C}$ dec. ^1H NMR (DMSO): δ 3.24 (s, 18H), 4.70 (AB system, 4H), 6.95 (m, 2H), 7.35–7.45 (m, 4H), 8.05 (d, 2H), 8.3 (s, 2H), 9.05 (s, 2H, acids). ^{13}C NMR ($\text{D}_2\text{O} + \text{DMSO}$): δ 53.99, 65.57, 115.67, 118.98, 124.90, 125.91, 129.48, 130.70, 130.59, 136.25, 138.06, 135.61. Anal. Calcd for $\text{C}_{28}\text{H}_{34}\text{I}_2\text{N}_2\text{O}_2$: C, 49.14; H, 5.01; I, 37.09; N, 4.09; O, 4.68. Found: C, 49.09; H, 5.11; N, 4.02.

Data for 3,5-Bis(dimethylaminomethyl)-4-hydroxybenzoic Acid Methyl Ester (3). White crystals. Mp: 61.0–61.6 $^\circ\text{C}$. ^1H NMR (DMSO): δ 2.22 (s, 12H), 3.56 (s, 4H), 3.78 (s, 3H), 7.69 (s, 2H), 8.7 (v br s, 1H). ^{13}C NMR (DMSO): δ 44.34, 51.55, 58.67, 118.96, 123.24, 129.40, 161.32, 166.21.

Data for 3,5-Bis[(trimethylammonium iodide)methyl]-4-hydroxybenzoic Acid Methyl Ester (4). White crystals. Mp: >209 $^\circ\text{C}$ dec. ^1H NMR (D_2O): δ 3.08 (s, 18H) 3.87 (s, 3H), 4.59 (s, 4H), 8.19 (s, 2H). ^{13}C NMR (D_2O): δ 53.04, 53.19, 64.11, 118.37, 122.84, 139.23, 161.86, 167.91.

Data for 2,6-Bis(dimethylaminomethyl)-4-methoxyphenol (5). Colorless oil. ^1H NMR (CDCl_3): δ 2.36 (s, 12H) 3.61 (s, 4H), 3.78 (s, 3H), 6.70 (s, 2H), 6.70 (s, 2H), 7.28 (s, 1H, acid). ^{13}C NMR (CDCl_3): δ 44.51, 55.68, 60.03, 114.41, 123.09, 150.42, 151.77.

Racemic 2,2'-Dihydroxy-3-(dimethylaminomethyl)-1,1'-binaphthyl (11). **Procedure A.** A solution of racemic 2,2'-dihydroxy-3-(*N,N*-dimethylcarbamoyl)-1,1'-binaphthyl (570 mg, 1.59 mmol) in dry THF (8 mL) was added slowly to a stirred suspension of LiAlH_4 (165 mg, 4.34 mmol) in dry THF (8 mL) at 0 $^\circ\text{C}$ under an inert atmosphere. The mixture was heated to reflux for 1 h, and then allowed to cool. The reaction was worked up by being stirred with 5 mL of saturated aqueous KF. The solution was extracted into 20 mL of DCM, washing the organic layer with 2×30 mL of brine, drying the organic layer with MgSO_4 , and removing the solvent to give a 96% yield of **11**, which could be used directly for the following step. Mp: >215 $^\circ\text{C}$ dec. ^1H NMR (CDCl_3): δ 2.44 (s, 6H) 3.95 (s, 2H), 5.14 (br s, 2H, D_2O exchangeable), 7.19–7.44 (m, 7H), 7.71 (s, 1H), 7.80–7.93 (m, 3H). ^{13}C NMR (CDCl_3): δ 43.85, 62.51, 112.17, 114.49, 117.14, 122.74, 123.17, 124.11, 124.14, 124.39, 125.97, 126.46, 127.34, 127.77, 127.87, 128.43, 128.84, 129.35, 133.20, 133.39, 150.96, 154.66. Anal. Calcd for $\text{C}_{23}\text{H}_{21}\text{NO}_2$: C, 80.44; H, 6.16; N, 4.08; O, 9.32. Found: C, 80.39; H, 6.18; N, 4.02.

Procedure B. A solution of racemic binol (500 mg, 1.75 mmol) in 2-methylpropan-1-ol (3.2 mL) and (isobutoxymethyl)dimethylamine (2.4 mL) was heated at 160 $^\circ\text{C}$ in a medium-pressure Pyrex reactor. After 17 h, the reaction mixture was cooled and a saturated solution of NH_4Cl (20 mL) was added. The solution was extracted with diethyl ether. The organic phase was extracted with HCl (5%), and NaHCO_3 was added to the aqueous solution to raise the pH to 7.8. The solution

(23) (a) Wesley, L. R. Eur. Pat. Appl. EP 42589 A1, 1981. (b) Moran, W. J.; Schreiber, E. C.; Engel, E.; Behn, D. C.; Yamins, J. L. *J. Am. Chem. Soc.* **1952**, *74*, 127–129. (c) Epstein, J.; Michel, H. O.; Rosenblat, P. H.; Plapinger, R. E.; Stephani, R. A.; Cook, E. *J. Am. Chem. Soc.* **1964**, *86*, 4959–4963.

was extracted twice with CH_2Cl_2 , and the organic phase was washed with water and dried over MgSO_4 . Evaporation of the solvent followed by column chromatography on silica gel (eluent ethyl acetate:methanol = 9:1) gave 0.375 g (1.09 mmol, 62% yield) of **11** as white crystals and 0.202 g (0.504 mmol, 29% yield) of **1**.

Racemic 2,2'-Dihydroxy-3-[(trimethylammonium iodide)methyl]-1,1'-binaphthyl (12). A solution of methyl iodide (0.2 mL 3.2 mmol) in dry acetonitrile (2 mL) was added to a solution of **11** (1.00 g 2.91 mmol) in dry acetonitrile (28 mL) at room temperature. The solution was left at room temperature for 6 h. After addition of 100 mL of diethyl ether, the insoluble quaternary ammonium salt was filtered to afford 1.36 mg of pure **12** (2.80 mmol, yield 96%). Mp: >254 °C dec. ^1H NMR (DMSO): δ 3.15 (s, 9H), 4.81 (s, 2H), 6.82–7.00 (m, 2H), 7.18–7.41 (m, 6H), 7.80–7.93 (m, 3H), 8.11 (s, 1H, D_2O exchangeable), 9.08 (s, 1H, D_2O exchangeable). ^{13}C NMR (DMSO): δ 52.70, 64.26, 113.14, 117.33, 118.20, 119.12, 123.05, 124.00, 124.14, 124.66, 126.82, 128.04, 128.09, 128.59, 128.77, 128.98, 130.39, 134.51, 135.32, 135.50, 152.05, 154.26. Anal. Calcd for $\text{C}_{24}\text{H}_{24}\text{INO}_2$: C, 59.39; H, 4.98; I, 26.15; N, 2.89; O, 6.59. Found: C, 59.14; H, 5.02; N, 2.85.

Photochemical Reactions. Irradiations were carried out by using 10 mL portions of the quinone methide precursors, the amines **1** and **11** (10^{-3} M) in CH_2Cl_2 and quaternary ammonium salts **2** and **12** (10^{-3} M) in water solutions, in Pyrex tubes. The tubes were capped after being flushed with argon for 5 min and externally irradiated by means of four 15 W phosphor-coated lamps (center of emission 310 nm) for 10 min and by means of four 15 W phosphor-coated lamps (center of emission 360 nm) for 25 min in a merry-go-round apparatus. Product formation was assessed by HPLC analysis.

Alkylation Adduct Isolation and Identification. The irradiated solution was evaporated under reduced pressure and the residue chromatographed on silica gel 60 HR by eluting with cyclohexanes–ethyl acetate or ethyl acetate–methanol mixtures. The adducts **7** and **10** have been identified by comparison with authentic samples.^{24a} The products were obtained as solids or oils from the fractions (by repeating the chromatography in the case of unsatisfactory separation) and characterized by NMR as detailed in the following.

Data for Racemic 3,3'-Bis[(octylthio)methyl]-1,1'-binaphthyl-2,2'-diol (6). Colorless oil. ^1H NMR (CDCl_3): δ 0.92 (t, 6H, $J = 7.0$ Hz), 1.20–1.35 (m, 16H), 1.37–1.48 (m, 4H), 1.54–1.71 (m, 4H), 2.51–2.62 (AB, 4H), 4.04 (s, 4H), 5.73 (s, 2H, acids), 7.05–7.12 (m, 2H), 7.22–7.31 (m, 2H), 7.32–7.44 (m, 2H), 7.82–7.97 (4H). ^{13}C NMR (CDCl_3): δ 13.63, 22.17, 28.47, 28.69, 28.75, 28.94, 31.32, 31.36, 31.47, 112.40, 123.67, 123.82, 126.22, 126.50, 127.55, 128.61, 130.10, 132.41, 150.80. Anal. Calcd for $\text{C}_{38}\text{H}_{50}\text{O}_2\text{S}_2$: C, 75.70; H, 8.36; O, 5.31; S, 10.64. Found: C, 75.44; H, 8.39; S, 10.58.

3,3'-Bis(2-methoxycarbonylpyrrolidin-1-ylmethyl)-1,1'-binaphthyl-2,2'-diol (8) is formed as a diastereomeric mixture of **8a** and **8b**.

Data for 8a. Colorless oil. ^1H NMR (CDCl_3): δ 1.87–2.07 (m, 4H), 2.16–2.28 (m, 2H), 2.57–2.65 (m, 2H), 3.14–3.21 (m, 2H), 3.49–3.54 (dd, 2H, $J = 4.8$ Hz, 8.7 Hz), 3.67 (s, 6H), 3.71–3.73 (m, 2H), 3.98 (d, 2H, $J = 13.3$ Hz), 4.37 (d, 2H, $J = 13.3$ Hz), 7.18–7.37 (m, 6H), 7.55 (s, 2H), 7.9 (d, 2H, $J = 7.7$ Hz). ^{13}C NMR (CDCl_3): δ 23.13, 29.40, 51.91, 52.55, 57.54, 64.68, 116.50, 122.70, 124.83, 125.09, 125.73, 127.32, 127.44, 128.05, 133.97, 153.24, 173.53. Anal. Calcd for $\text{C}_{34}\text{H}_{36}\text{N}_2\text{O}_6$: C, 71.81; H, 6.38; N, 4.93; O, 16.88. Found: C, 71.69; H, 6.43; N, 4.91.

Data for 8b. Colorless oil. ^1H NMR (CDCl_3): δ 1.83–2.01 (m, 4H), 2.19–2.26 (m, 2H), 2.54–2.62 (m, 2H), 3.08–3.15 (m, 2H), 3.41–3.46 (dd, 2H, $J = 6.2$ Hz, 9.1 Hz), 3.67 (s, 6H), 3.70–3.73 (m, 8H), 3.81 (d, 2H, $J = 13.1$ Hz), 4.51 (d, 2H, $J = 13.1$ Hz), 7.14–7.28 (m, 6H), 7.66 (s, 2H), 7.70 (d, 2H, $J = 7.7$ Hz). ^{13}C NMR (CDCl_3): δ

23.10, 29.43, 52.05, 52.71, 57.75, 65.19, 116.40, 122.68, 124.64, 124.99, 125.78, 127.43, 127.54, 128.08, 133.97, 153.25, 173.46. Anal. Calcd for $\text{C}_{34}\text{H}_{36}\text{N}_2\text{O}_6$: C, 71.81; H, 6.38; N, 4.93; O, 16.88. Found: C, 71.49; H, 6.40; N, 4.88.

Data for Racemic 3,3'-Bis(2-hydroxyethylsulfanylmethyl)-1,1'-binaphthyl-2,2'-diol (9). Colorless oil. ^1H NMR (CDCl_3): δ 2.28 (br s, 2H, acids), 2.71–2.91 (m, 4H), 3.62–3.78 (m, 4H), 4.01 (d, 2H, $J = 13.0$ Hz), 4.13 (d, 2H, $J = 13.0$ Hz), 6.20 (br s, 2H, acids), 7.30 (m, 2H), 7.50 (m, 2H), 7.55 (m, 2H), 7.8–8.0 (m, 4H). ^{13}C NMR (CDCl_3): δ 30.56, 33.94, 59.86, 111.78, 123.38, 123.44, 126.29, 126.44, 127.11, 128.18, 129.95, 132.16, 150.26. Anal. Calcd for $\text{C}_{26}\text{H}_{26}\text{O}_4\text{S}_2$: C, 66.92; H, 5.62; O, 13.72; S, 13.74. Found: C, 66.74; H, 5.73; S, 13.63.

Data for Racemic 3-(2-Hydroxyethylsulfanylmethyl)-1,1'-binaphthyl-2,2'-diol (14). Colorless oil. ^1H NMR (CDCl_3): δ 2.45 (br s, 2H, acids), 2.79–2.90 (m, 2H), 3.68–3.79 (m, 2H), 4.0 (AB system, 2H, $J = 7.7$ Hz), 7.09–7.15 (m, 2H), 7.28–7.46 (m, 5H), 7.83–8.05 (m, 4H), 8.96 (br s, 2H, acids). ^{13}C NMR (CDCl_3): δ 31.17, 34.75, 60.53, 110.85, 112.14, 117.83, 123.76, 123.98, 124.14, 124.19, 126.95, 127.07, 127.21, 127.82, 128.20, 128.98, 129.21, 130.69, 131.19, 132.78, 133.28, 150.83, 152.66. Anal. Calcd for $\text{C}_{23}\text{H}_{20}\text{O}_3\text{S}$: C, 73.38; H, 5.35; O, 12.75; S, 8.52. Found: C, 73.26; H, 5.40; S, 8.46.

3-[2-(2-Amino-2-methoxycarbonylethylsulfanylmethyl)-1,1'-binaphthyl-2,2'-diol (15) is formed as a diastereomeric mixture of **15a** and **15b**.

Data for 15a. Colorless oil. ^1H NMR (CDCl_3): δ 2.92–3.00 (dd, 1H, $J = 14.9$ Hz, $J = 8.20$ Hz), 3.33–3.38 (dd, 1H, $J = 14.9$ Hz, $J = 3.8$ Hz), 4.09–4.18 (m, 2H), 4.22–4.26 (dd, 1H, $J = 8.2$ Hz, $J = 3.8$ Hz), 6.55 (br s, 2H, acids), 6.99–7.43 (m, 7H), 7.71–7.96 (m, 4H). ^{13}C NMR (CDCl_3): δ 31.36, 31.83, 52.33, 53.51, 111.01, 114.73, 118.05, 123.80, 124.10, 124.44, 124.65, 125.53, 127.19, 127.29, 127.84, 128.29, 128.81, 129.22, 130.49, 131.30, 133.30, 133.71, 149.39, 152.62, 167.61. Anal. Calcd for $\text{C}_{25}\text{H}_{23}\text{NO}_4\text{S}$: C, 69.26; H, 5.35; N, 3.23; O, 14.76; S, 7.40. Found: C, 69.19; H, 5.42; N, 3.21; S, 7.34.

Data for 15b. Colorless oil. ^1H NMR (CDCl_3): δ 3.11–3.13 (m, 2H), 3.72–3.76 (m, 1H), 3.89–3.98 (m, 2H), 6.55 (br s, 2H, acids), 7.00–7.43 (m, 7H), 7.71–7.98 (m, 4H). ^{13}C NMR (CDCl_3): δ 31.94, 32.82, 52.51, 53.57, 111.01, 115.21, 117.98, 123.80, 124.10, 124.44, 124.65, 125.53, 127.19, 127.26, 127.77, 128.29, 128.98, 129.17, 130.57, 131.35, 133.18, 133.65, 149.30, 152.55, 167.74. Anal. Calcd for $\text{C}_{25}\text{H}_{23}\text{NO}_4\text{S}$: C, 69.26; H, 5.35; N, 3.23; O, 14.76; S, 7.40. Found: C, 69.14; H, 5.40; N, 3.18; S, 7.30.

3-(2-Methoxycarbonylpyrrolidin-1-ylmethyl)-1,1'-binaphthyl-2,2'-diol (16) is formed as a diastereomeric mixture of **16a** and **16b**.

Data for 16a. ^1H NMR (CDCl_3): δ 1.85–1.99 (m, 2H), 2.00–2.04 (m, 1H), 2.21–2.29 (m, 1H), 2.60–2.63 (m, 1H), 3.22–3.26 (m, 1H), 3.46–3.51 (m, 1H), 3.50 (s, 3H), 4.12 (d, 1H, $J = 14.7$ Hz), 4.19 (d, 1H, $J = 14.7$ Hz), 7.13–7.44 (m, 6H), 7.70–7.96 (m, 5H, + 2H acids). ^{13}C NMR (CDCl_3): δ 23.03, 29.61, 52.00, 53.64, 57.97, 65.03, 113.41, 118.00, 122.82, 123.42, 123.65, 123.86, 124.47, 124.75, 126.05, 126.55, 127.35, 127.62, 127.89, 128.16, 128.92, 129.01, 129.58, 130.43, 133.81, 151.69, 173.77. Anal. Calcd for $\text{C}_{27}\text{H}_{25}\text{NO}_4$: C, 75.86; H, 5.89; N, 3.28; O, 14.97. Found: C, 75.71; H, 5.94; N, 3.22.

Data for 16b. ^1H NMR (CDCl_3): δ 1.86–2.00 (m, 2H), 2.00–2.04 (m, 1H), 2.21–2.29 (m, 1H), 2.55–2.57 (m, 1H), 3.10–3.20 (m, 1H), 3.34–3.40 (m, 1H), 3.68 (s, 3H), 3.87 (d, 1H, $J = 13.2$ Hz), 4.48 (d, 1H, $J = 13.2$ Hz), 7.13–7.44 (m, 6H), 7.70–7.96 (m, 5H, + 2H acids). ^{13}C NMR (CDCl_3): δ 23.03, 29.29, 52.09, 52.89, 57.31, 65.66, 114.84, 117.45, 122.98, 123.46, 123.73, 124.11, 124.72, 125.00, 126.12, 127.07, 127.16, 127.50, 127.95, 128.17, 128.56, 129.06, 129.46, 131.06, 133.64, 151.15, 173.18. Anal. Calcd for $\text{C}_{27}\text{H}_{25}\text{NO}_4$: C, 75.86; H, 5.89; N, 3.28; O, 14.97. Found: C, 75.67; H, 6.01; N, 3.19.

The alkylation adducts **7**,²⁴ **10**,^{24a} **13**,^{24a} and **17**^{24a} were previously reported and were recognized either by comparison with an authentic sample or by comparison of the ^1H and ^{13}C NMR spectroscopic data.

(24) Cram, D. J.; Helgeson, R. C.; Peacock, S. C.; Kaplan, L. J.; Domeir, L. A.; Moreau, P.; Koga, K.; Mayer, J. M.; Chao, J.; Siegel, M. G.; Hoffman, D. H.; Dotsevi Sogah, G. Y. *J. Org. Chem.* **1978**, *43*, 1930–1946. (b) Sone, T.; Kobori, Y.; Ando, Y.; Ohba, Y. *Bull. Chem. Soc. Jpn.* **1994**, *67*, 3366–3369.

Flash Photolysis. The laser flash photolysis studies were carried out by using the fourth (266 nm) and the third (356 nm) harmonics of a Q-switched Nd:YAG laser (model HY 200, JK Laser Ltd. Lumonics). This delivered 3 mJ pulses with a duration of ca. 10 ns. The monitor system, arranged in crossbeam configuration, consisted of a laser kinetic spectrophotometer (model K 347, Applied Photophysics) fitted with a 200 W Xe arc lamp, an F/3.4 monochromator, and a five-stage photomultiplier. The signals were captured by a Hewlett-Packard 54510A digitizing oscilloscope, and the data were processed on a 286-based computer system using software developed by Prof. C. Long (Dublin) and modified by Prof. Mauro Freccero.

Computational Details. All calculations were carried out using the Gaussian 98²⁵ and 2003²⁶ (for solvent optimization) program packages. All the geometric structures of reactant **2** (two conformers, **2a** and **2b**) and the *para*-unsubstituted analogue of **4** (**4H**) (Scheme 3, Y = H) were fully optimized in the gas phase and in water solution using the hybrid density functional method B3LYP with the 6-31G(d) basis set. The bulk solvent effects on the geometries and energies of the reactants were calculated via the self-consistent reaction field (SCRF) method using the conductor version of PCM (C-PCM)²⁷ as implemented in the B.05 version of Gaussian 2003. The cavity is composed by

interlocking spheres centered on non-hydrogen atoms with radii obtained by the HF parametrization of Barone known as the united atom topological model (UAHF).²⁸ Such a model includes the non-electrostatic terms (cavitation, dispersion, and repulsion energy) in addition to the classical electrostatic contribution.

Gel Electrophoresis. Plasmid pBR322 (0.5 $\mu\text{g}/\text{sample}$) in its circular (90%) and linear (10%) forms was mixed with increasing amounts (0.5, 1, 5, 10, and 50 μM) of compounds **2–5** in phosphate buffer (50 mM, pH 7.5). A saturated water solution of 4,5',8-trimethylpsoralen was used to obtain a 0.5 nM concentration of drug in the control samples. Reaction mixtures were irradiated for 30 min at room temperature at 360 nm. Irradiated solutions were added of alkaline agarose gel loading buffer (50 mM NaOH, 1 mM EDTA, 3% Ficoll, 0.02% bromophenol blue) and loaded onto a 1% alkaline agarose gel containing 50 mM NaOH and 1 mM EDTA. Gels were run in 50 mM NaOH and 1 mM EDTA at 100 mA for 18 h, stained with ethidium bromide (0.5 $\mu\text{g}/\text{mL}$) for 30 min, and subsequently washed in water for 30 min. Stained gels were visualized in Gel-Doc 1000 (Bio-Rad, Italy), and DNA bands were quantified by Quantity One software (Bio-Rad). For pH-dependent activity, **2** (10 μM), **3** (50 μM), and **4** (10 μM) were mixed with pBR322 in phosphate-buffered solutions at pH 6.5, 7.5, or 8.8. For wavelength-dependent DNA cross-linking activity, **2–5** at concentrations of 10 and 100 μM were mixed with pBR322 in phosphate-buffered solutions at pH 7.5. Solutions were irradiated for 30 min at 360 or 310 nm.

Acknowledgment. This research was supported in part by Pavia University (Grant FAR 2002).

Supporting Information Available: Energies and Cartesian coordinates of stationary points of **2a**, **2b**, and **4H** in Figure 5 in the gas phase and in water solution, optimized at the B3LYP/6-31G(d) level of theory (PDF). This material is available free of charge via the Internet at <http://pubs.acs.org>.

JA047655A

- (25) Frisch, M. J.; Trucks, G. W.; Schlegel, H. B.; Scuseria, G. E.; Robb, M. A.; Cheeseman, J. R.; Zakrzewski, V. G.; Montgomery, J. A., Jr.; Stratmann, R. E.; Burant, J. C.; Dapprich, S.; Millam, J. M.; Daniels, A. D.; Kudin, K. N.; Strain, M. C.; Farkas, O.; Tomasi, J.; Barone, V.; Cossi, M.; Cammi, R.; Mennucci, B.; Pomelli, C.; Adamo, C.; Clifford, S.; Ochterski, J.; Petersson, G. A.; Ayala, P. Y.; Cui, Q.; Morokuma, K.; Malick, D. K.; Rabuck, A. D.; Raghavachari, K.; Foresman, J. B.; Cioslowski, J.; Ortiz, J. V.; Stefanov, B. B.; Liu, G.; Liashenko, A.; Piskorz, P.; Komaromi, I.; Gomperts, R.; Martin, R. L.; Fox, D. J.; Keith, T.; Al-Laham, M. A.; Peng, C. Y.; Nanayakkara, A.; Gonzalez, C.; Challacombe, M.; Gill, P. M. W.; Johnson, B. G.; Chen, W.; Wong, M. W.; Andres, J. L.; Head-Gordon, M.; Replogle, E. S.; Pople, J. A. *Gaussian 98*, revision A.11.2; Gaussian, Inc.: Pittsburgh, PA, 1998.
- (26) Frisch, M. J.; Trucks, G. W.; Schlegel, H. B.; Scuseria, G. E.; Robb, M. A.; Cheeseman, J. R.; Montgomery, J. A., Jr.; Vreven, T.; Kudin, K. N.; Burant, J. C.; Millam, J. M.; Iyengar, S. S.; Tomasi, J.; Barone, V.; Mennucci, B.; Cossi, M.; Scalmani, G.; Rega, N.; Petersson, G. A.; Nakatsuji, H.; Hada, M.; Ehara, M.; Toyota, K.; Fukuda, R.; Hasegawa, J.; Ishida, M.; Nakajima, T.; Honda, Y.; Kitao, O.; Nakai, H.; Klene, M.; Li, X.; Knox, J. E.; Hratchian, H. P.; Cross, J. B.; Adamo, C.; Jaramillo, J.; Gomperts, R.; Stratmann, R. E.; Yazyev, O.; Austin, A. J.; Cammi, R.; Pomelli, C.; Ochterski, J. W.; Ayala, P. Y.; Morokuma, K.; Voth, G. A.; Salvador, P.; Dannenberg, J. J.; Zakrzewski, V. G.; Dapprich, S.; Daniels, A. D.; Strain, M. C.; Farkas, O.; Malick, D. K.; Rabuck, A. D.; Raghavachari, K.; Foresman, J. B.; Ortiz, J. V.; Cui, Q.; Baboul, A. G.; Clifford, S.; Cioslowski, J.; Stefanov, B. B.; Liu, G.; Liashenko, A.; Piskorz, P.; Komaromi, I.; Martin, R. L.; Fox, D. J.; Keith, T.; Al-Laham, M. A.; Peng, C. Y.; Nanayakkara, A.; Challacombe, M.; Gill, P. M. W.; Johnson, B. G.; Chen, W.; Wong, M. W.; Gonzalez, C.; Pople, J. A. *Gaussian 03*, revision B.05; Gaussian, Inc.: Pittsburgh, PA, 2003.
- (27) (a) Becke, A. D. *J. Chem. Phys.* **1993**, *98*, 1372–1377. (b) Schmider, H. L.; Becke, A. D. *J. Chem. Phys.* **1998**, *108*, 9624–9631.
- (28) (a) Barone, V.; Cossi, M. *J. Phys. Chem. A* **1998**, *102*, 1995–2001. For the original COSMO model see: (b) Klamt, A.; Schüürmann, G. *J. Chem. Soc., Perkins Trans. 2* **1993**, 799–805. (c) Klamt, A.; Jonas, V.; Bürger, T.; Lohrenz, J. C. W. *J. Phys. Chem. A* **1998**, *102*, 5074–5085. For a more comprehensive treatment of solvation models see: (d) Cramer, C. J.; Truhlar, D. G. *Chem. Rev.* **1999**, *99*, 2161–2200.
- (29) Douki, T.; Angelov, D.; Cadet, J. *J. Am. Chem. Soc.* **2001**, *123*, 11360–11366.